Thin Solid Films 529 (2013) 190–194

Contents lists available at SciVerse ScienceDirect

Thin Solid Films

journal homepage: www.elsevier.com/locate/tsf

Temperature-dependent electrical and photo-sensing properties of horizontally-oriented carbon nanotube networks synthesized by sandwich-growth microwave plasma chemical vapor deposition

I-Ju Teng [a,e], Hui-Lin Hsu [b], Sheng-Rui Jian [c,*], Li-Chun Wang [a], Kai-Ling Chen [a], Cheng-Tzu Kuo [a,*], Fu-Ming Pan [a], Wei-Hsiang Wang [d], Jenh-Yih Juang [e]

[a] Department of Materials Science and Engineering, National Chiao Tung University, Hsinchu 30010, Taiwan
[b] Department of Electrical and Computer Engineering, University of Toronto, Toronto M5S 3G4, Canada
[c] Department of Materials Science and Engineering, I-Shou University, Kaohsiung 84041, Taiwan
[d] Teraxtal Technology Corporation, Hsinchu 30075, Taiwan
[e] Department of Electrophysics, National Chiao Tung University, Hsinchu 30010, Taiwan

ARTICLE INFO

Available online 17 September 2012

Keywords:
Electrical properties
Photo-sensing properties
Carbon nanotube networks (CNT-NWs)
CNT-NW-assisted devices
Microwave plasma chemical vapor deposition
Sandwich-growth
Horizontally-oriented interconnected

ABSTRACT

The electrical and photo-sensing properties of horizontally-oriented interconnected carbon nanotube networks (CNT-NWs) prepared by means of a microwave plasma chemical vapor deposition sandwich-growth process are investigated. The temperature-dependent dark and illuminated current–voltage and transfer characteristics of CNT-NW-assisted devices are measured. Results show that the current–voltage characteristics of the devices exhibit nonlinear behavior, and the current can be further modulated by a gate voltage, revealing *p*-type semiconducting behavior with a device mobility of ~14.5 $cm^2/V \cdot s$ and an on-off current ratio of ~10^3. Moreover, when the CNT-NW-assisted devices are irradiated with 1.25–25 μm infrared (IR) from 300 to 11 K, the photo currents increase approximately 1.1- to 2.7-fold compared to the dark currents at ±2 V bias voltage. Such results demonstrate that the presented CNT-NWs have high potential for IR photo-sensor applications.

1. Introduction

Recently, devices based on networks of carbon nanotubes (CNTs) have attracted considerable research attention [1–9] owing to their potential in overcoming some of the technological challenges involved in the integration of single nanotube devices into scalable integrated circuits. One of the main challenging issues being still encountered in nanotube electronics research society is the chirality, position and orientation control of the individual nanotube [1–3]. Another important challenge is the limited current-carrying capacities and number of conduction channels as well as poor reproducible properties from single nanotube devices [1,2,4,5]. The use of nanotube-network-based structures provides an attractive alternative to avoid these challenges while retaining the remarkable properties of individual CNTs as well as providing processing capabilities of mass fabrication techniques [1,2,10–16]. Furthermore, this type of carbon nanostructures would have the additional advantage of ensuring a simple device fabrication process or even possible to directly employ as-produced carbon nanotube network (CNT-NW) samples to fabricate large-scale integrated devices, including sensors, flexible transistors, and integrated circuits [1–7,10,22].

A wide variety of methods have been demonstrated to fabricate CNT-NWs [1,2]. Among them, chemical vapor deposition (CVD) offers the low-cost mass-production processing for directly obtaining pristine "high-purity" CNT-NWs on insulating surfaces without the need for acid cleaning or any complicated chemical and printing procedures [3–5,17–19]. More importantly, the CVD technique also provides good control over the tube density, morphology, alignment, and position, which is important as these parameters significantly influence the collective properties of CNTs [3–5,17–19]. However, due to the required relatively high growth temperature (>800 °C), the long process time (several tens of minutes), and always incorporation of pre-patterned catalysts/substrates for carrying out directed growth strategies, current CVD procedures for synthesizing CNT-NWs are still incompatible for direct integration into microelectronics processing [3–5,17–19].

A sandwich-growth microwave plasma chemical vapor deposition (MPCVD) method for direct growth of horizontally-oriented interconnected CNT-NWs on unpatterned substrates at relatively low temperatures (≤600 °C) with short time process (4–6 min) was reported previously [20]. Here, we further demonstrate that the proposed CNT-NW growth technology indeed opens potential and immediate possibilities for natural integration of such unique

* Corresponding authors.
E-mail addresses: srjian@gmail.com (S.-R. Jian), kurt.kuotw@gmail.com (C.-T. Kuo).

0040-6090/$ – see front matter © 2012 Elsevier B.V. All rights reserved.
http://dx.doi.org/10.1016/j.tsf.2012.09.019

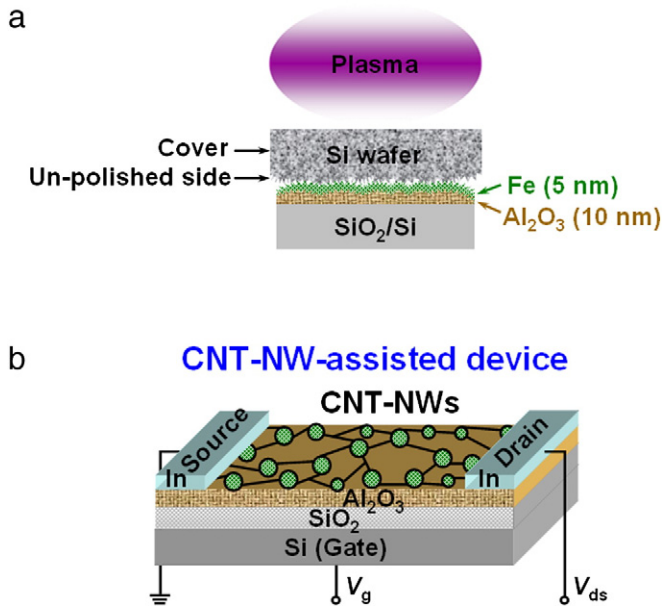

Fig. 1. (a) Schematic illustration of the sandwiched specimen stack structure used in this work for direct growth of horizontally-oriented interconnected CNT-NWs. (b) Schematic picture of a CNT-NW-assisted device.

carbon nanostructures into specialized devices by directly employing as-grown samples to fabricate simple CNT-NW-assisted devices. Then, we use such devices to investigate the electrical and photo-sensing properties of the CNT-NWs by current–voltage measurement in dark and under illumination conditions at various temperatures.

2. Experimental details

2.1. CNT-NW growth

Fig. 1(a) shows a schematic diagram of the sandwiched specimen stack structure [20] used in this work for direct growth of horizontally-oriented interconnected CNT-NWs. A SiO_2 layer of 500 nm was thermally grown on a Si wafer followed by an Al_2O_3 layer of 10 nm and a Fe catalyst film with a thickness of 5 nm deposition sequentially. The Fe film and Al_2O_3 layer were both prepared by sputtering. The coated Si substrate was then covered by another Si wafer during the deposition process. Such a stacked structure was designed to restrict the gas flow direction and to suppress the damages on the catalyst and/or growing tubes resulting from the ion bombardment of plasma. It is also advantageous for preventing catalyst particles from being poisoned by excess carbon species or amorphous carbon deposits during growth. The sandwiched structure was then pretreated by hydrogen plasma operated with parameters of 100 sccm H_2, chamber pressure of ~4 kPa, and plasma power of 400 W for 15 min in MPCVD. After pretreatment, CH_4 was subsequently introduced into MPCVD to initiate CNT-NW growth at a total gas pressure of ~2.2 kPa and plasma power of 750 W for 6 min growth time with CH_4/H_2 ratio of 1.5/400 sccm/sccm. There is no additional heater installed on the substrate holder of our MPCVD system. The substrate holder was heated directly by the plasma, and the sample temperature was slightly varied in the range from 594 to 597 °C monitored by the thermocouples embedded inside the substrate holder. After growth, the samples were analyzed using a JEOL JSM-6500F field-emission scanning electron microscope (FESEM) operating at 15 kV, a JEOL JEM-2100F high-resolution transmission electron microscope (HRTEM) operating at 200 kV, and a micro-Raman spectrometer (Renishaw RM-1000, excitation laser: 514.5 nm in wavelength, laser spot: ~5 μm in diameter).

2.2. CNT-NW-assisted device fabrication and measurements

We directly employed as-grown samples to fabricate simple CNT-NW-assisted devices. Two indium (In) metal strips were directly soldered on the top surface of the samples to serve as the source and drain electrodes. The heavily doped Si substrate was utilized as the bottom gate electrode, with 500 nm thermally grown SiO_2 on top as the gate dielectric, as depicted schematically in Fig. 1(b). The distance between the central (voltage) strips (L_c) was about 100 μm with the strip width (W_s) of ~200 μm. The dark and illuminated current–voltage (I_{ds} (source-drain current)–V_{ds} (source-drain voltage)) and transfer characteristics (I_{ds}–V_g (gate voltage)) of the CNT-NW-assisted devices were measured in vacuum (~10^{-5} Pa) and in air at 11–300 K using a semiconductor Agilent parameter analyzer (HP4156B) and an infrared (IR) source provided by the Fourier Transform IR spectroscopy. The IR radiation covered the wavelength range of 1.25–25 μm. Each measurement was repeated several times to ensure that the data were indeed reproducible.

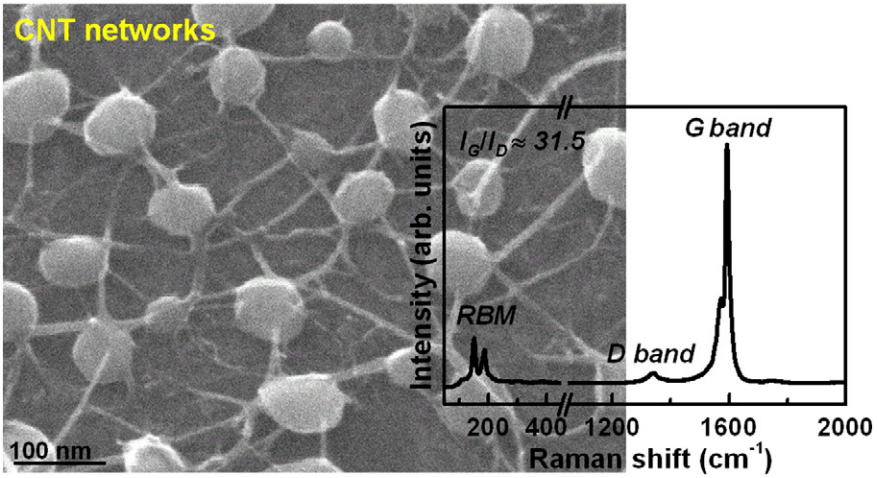

Fig. 2. FESEM image of the as-grown CNT-NWs synthesized by our MPCVD sandwich-growth process. The inset shows the Raman spectra for the CNT-NWs, obtained using the 514.5 nm line of an Ar laser.

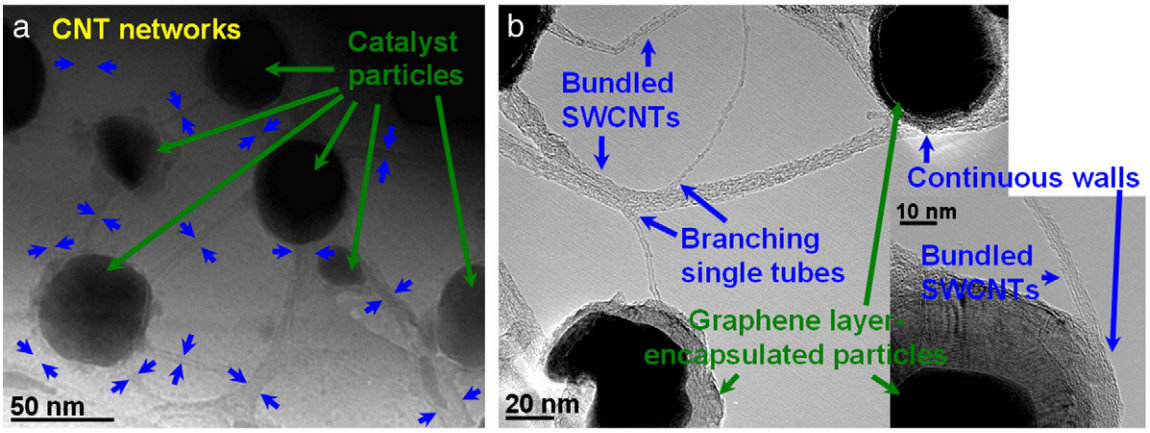

Fig. 3. (a) Low magnification TEM image of the CNT-NWs. (b) HRTEM image of the SWCNTs grown from the graphene layer-encapsulated particles. Inset: higher-magnification image of an individual scale.

3. Results and discussion

3.1. Morphology and structure characterization of CNT-NWs

Fig. 2 displays the FESEM image of the CNT-NWs grown on an Al_2O_3-coated SiO_2/Si substrate with 5 nm thick Fe catalyst. It reveals that the obtained "film" comprises dispersed large-diameter catalyst particles (~45–100 nm) connected by surface-grown CNTs to develop the structure of horizontally-oriented interconnected CNT-NWs. We further use Raman spectroscopy to evaluate the quality of the CNT-NWs. As shown in the inset of Fig. 2, the significant radial breathing mode (RBM) signals and G-band peaks can evidently demonstrate the existence of single- or double-walled nanotubes within the CNT-NWs [21]. Furthermore, the high I_G/I_D ratio (~31.5) indicates that the as-grown CNT-NWs are of highly-crystallinity (purity and good quality) [21].

The structure and diameter of the CNT-NWs are further characterized by using HRTEM. The HRTEM images, shown in Fig. 3(a), reveal that the CNTs are grown from the specific sites of particles and then connected with neighboring particles/tubes to develop an interconnected network. Fig. 3(b) and its inset further display that the CNT-NWs consist of a mixture of graphene layer-encapsulated particles and interconnected single-walled carbon nanotubes (SWCNTs), isolated or branched or assembled into bundles; of which SWCNTs stick out from the outermost shell of graphene layer-encapsulated particles, behaving as continuous walls, and finally attach to surrounding particles/tubes. The main reason to form such unique networks may be due to the sandwiched effect of two rougher surfaces of the Al_2O_3 layer and the covering Si wafer; however, details of the formation mechanism of the CNT-NWs synthesized by the proposed sandwich-growth MPCVD method need further verification.

3.2. Electrical and photo-sensing properties of CNT-NW-assisted devices

To evaluate the feasibility of using the CNT-NWs as active materials for electronic devices, the electrical properties of CNT-NW-assisted devices are investigated by the measurement of temperature-dependent I_{ds}–V_{ds} and transfer characteristics I_{ds}–V_g. Fig. 4 shows the I_{ds}–V_{ds} curves obtained from several different devices measured in a vacuum probe station at 11–300 K. As shown, the I_{ds}–V_{ds} curves show nonlinear properties at all temperatures, and the nonlinearities in the I_{ds}–V_{ds} curves become more pronounced as temperature decreases. The current level for the devices measured under air at fixed source-drain bias conditions is similar to that obtained under vacuum, as displayed in the lower right inset of Fig. 4 for the case of 300 K. The nonlinear nature of the I_{ds}–V_{ds} curves indicates that Schottky barriers might be formed at the interface of the metal and tube contacts as well as at the junctions of semiconducting and metallic tubes [22–24].

We further study the transfer characteristics of the CNT-NW-assisted devices to understand the effect of a V_g on the I_{ds} of the devices. The V_g dependence of I_{ds} under a certain V_{ds} of 0.1 V measured at 300 K in air is displayed in the upper left inset of Fig. 4. As displayed, the I_{ds} is quenched for positive V_g with an on–off current ratio of about 10^3, indicating that the CNT-NW-assisted devices exhibit *p*-type semiconductor characteristics. Such *p*-type behavior of CNT-based devices has been mostly ascribed to the adsorption of atmospheric oxygen resulting in either *p*-doping [25–28] or work function increase [29,30]. Since our devices are fabricated without taking any care to avoid from exposure to air, it is natural to assume that the measured samples might be with possible oxygen adsorption. The high on–off ratio also implies that there should be no pathways of solely metallic nanotubes in the CNT-NWs; that is, the less-abundant metallic tubes might play a role only as interconnects between the semiconducting tubes that determine the semiconducting characteristics in the total conductance of the networks [2,3,5,22]. Additionally, we use the standard formula [3,4,24,31], $\mu_{eff} = \left(\frac{dI_{ds}}{dV_g}\right)\frac{d_{ox}L_c}{\varepsilon V_{ds} W_s}$, to

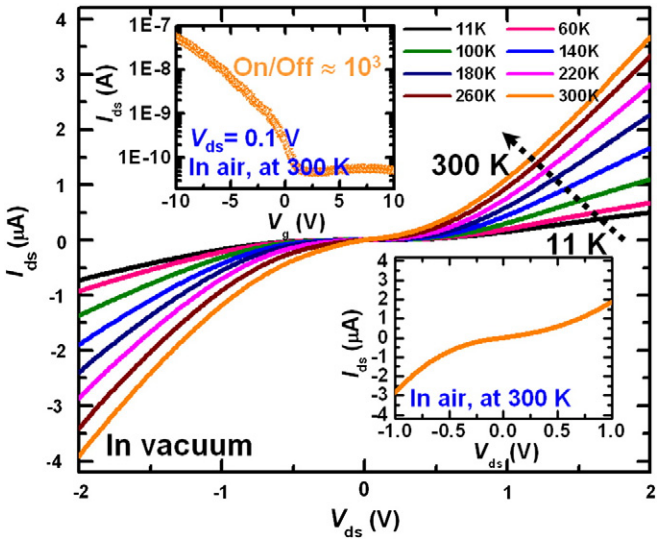

Fig. 4. I_{ds}–V_{ds} characteristics of the CNT-NW-assisted devices, measured in vacuum at temperatures ranging from 11 to 300 K. Upper left inset: transfer characteristics of the CNT-NW-assisted devices, plotted on a logarithmic scale, at V_{ds} = 0.1 V. Lower right inset: I_{ds}–V_{ds} characteristics measured at 300 K in ambient air for the CNT-NW-assisted devices.

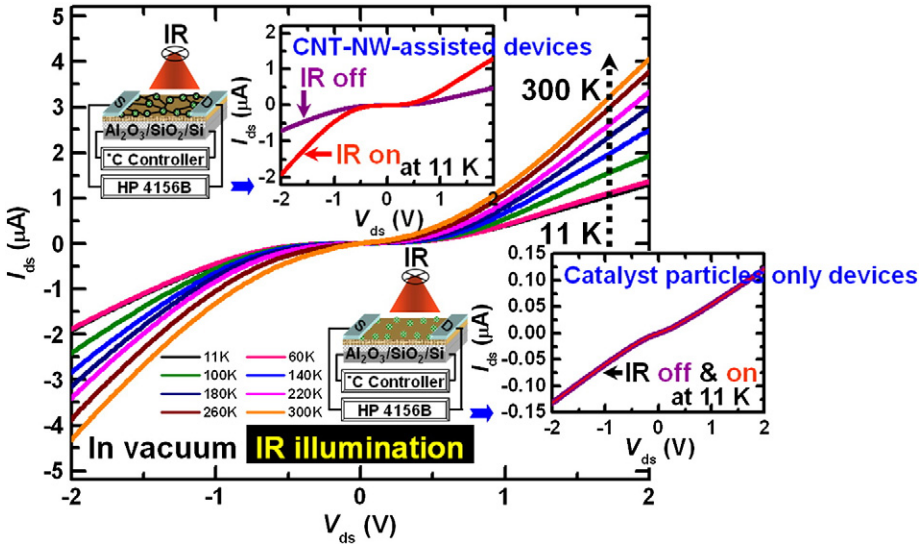

Fig. 5. Photocurrent response of the CNT-NW-assisted devices under IR light irradiation measured between 11 K and 300 K under vacuum. Insets: examples of the effect of the IR illumination at 11 K on CNT-NW-assisted devices (upper figure) and catalyst particles only devices (lower figure), respectively, with corresponding schematic diagrams of the measurement setup.

estimate an effective mobility of our CNT-NW-assisted devices, where the thickness (d_{ox}) and dielectric constant (ε) of the SiO_2 gate oxide are 500 nm and 3.9, respectively. Accordingly, the effective mobility (μ_{eff}) in our devices is approximately 14.5 $cm^2/V \cdot s$, which is a typical value for devices made of networked CNTs [2–4,24,31]. The experimental observations suggest that the CNT-NWs may be a viable material for transistor applications. Importantly, the layout of such CNT-NWs offers the opportunities to achieve high on–off ratio and uniform mobility without further processing steps for the selective removal of metallic nanotubes. However, further studies to optimize the device performance and to explore the electrical transport properties being possibly inherent in such unique networks are needed. Work is currently underway in our group.

Regarding the photo-sensing capabilities of the CNT-NW-assisted devices, the responses of the devices under IR illumination are studied. Fig. 5 shows the temperature-dependent I_{ds}–V_{ds} characteristics of the devices illuminated using an IR source with wavelength of 1.25–25 μm being incident normally to the sample surface. The insets show examples of the effect of the IR radiation at 11 K on the CNT-NW-assisted devices and catalyst particles only devices, respectively, with the corresponding schematic diagrams of the measurement setup. All of the tests are carried out under vacuum to minimize the effect of gas molecules. As indicated in Fig. 5, the photocurrents induced at 11 to 300 K vary from 1.9 to 4.4 μA at the bias voltage of ±2 V for the CNT-NW-assisted devices. Furthermore, it can be found from the figure shown in the upper left inset that when the CNT-NW-assisted devices are irradiated by the IR light, a dramatic increase in photocurrent from a dark value of 0.71 μA to 1.92 μA can be clearly observed at 11 K, indicating a 2.7-fold increased photocurrent. The increase in the IR illumination-induced photocurrents is in fact observable over the entire temperature range measured. This would be presumably due to the absorption of photon energy by the nanotubes, resulting in generation of electron–hole pairs or excitons and subsequent charge separation by the electrical field before recombination [15,32]. In contrast, for devices built with catalyst particles only, no noticeable variations in photocurrents can be detected at ±2 V bias voltage, as displayed in the lower right inset of Fig. 5, indicating that the catalyst particles only devices could not be used for photo-sensing, whereas the CNT-NWs would act as the important component for light detection in this case. Although further investigations are required to elucidate the photoresponse mechanisms involved in such CNT-NW-assisted devices, and to obtain optimal device performance, the preliminary data have shown that the horizontally-oriented interconnected CNT-NWs are distinctive structures with potential uses for photo-sensors.

4. Conclusions

Horizontally-oriented interconnected CNT-NWs are directly synthesized on unpatterned Si substrates by a sandwich-growth technology in MPCVD. The as-grown samples can also be directly integrated into simple CNT-NW-assisted devices for electrical and photo-sensing characterization of the CNT-NWs. The transfer characteristics of the CNT-NW-assisted devices exhibit *p*-type semiconducting behavior with promising device performance, including a ~10^3 of on-off ratio and ~14.5 $cm^2/V \cdot s$ of field effect mobility. Moreover, the photocurrent responses of the same devices show that significant IR illumination-induced photocurrents can be detected in the entire measured temperature range of 11–300 K at the bias voltage of ±2 V. The fact that no detectable photocurrent change is witnessed for the devices built with catalyst particles only suggests the prominent role played by the CNT-NWs for photo-sensing. We believe that the present achievement opens the way for future development of effective transistors and photo-detectors based on the CNT-NWs.

Acknowledgments

This work was supported by Taiwan National Science Council under project numbers NSC100-2221-E-214-024 and NSC99-2112-M-214-001, and by MOE ATU program at NCTU. The authors acknowledge the MSE department, CNST and NFC at NCTU, and CSIST for facility supports, and acknowledge valuable discussions with Dr. Shiang-Feng Tang, Terry Tai-Jui Wang, and Jung-Hsuan Chen.

References

[1] B.Y. Lee, M.G. Sung, H. Lee, S. Namgung, S.Y. Park, D.S. Choi, S. Hong, NPG Asia Mater. 2 (3) (2010) 103 (and references therein).
[2] Q. Cao, J.A. Rogers, Adv. Mater. 21 (2009) 29 (and references therein).
[3] U.J. Kim, E.H. Lee, J.M. Kim, Y.S. Min, E. Kim, W. Park, Nanotechnology 20 (2009) 295201 (and references therein).
[4] E.S. Snow, J.P. Novak, P.M. Campbell, D. Park, Appl. Phys. Lett. 82 (2003) 2145.
[5] J.P. Edgeworth, N.R. Wilson, J.V. Macpherson, Small 3 (2007) 860.
[6] L.C. Wang, K.T. Tang, I.J. Teng, C.T. Kuo, C.L. Ho, H.W. Kuo, T.H. Su, S.R. Yang, G.N. Shi, C.P. Chang, Sensors 11 (2011) 7763.

[7] G. Peng, U. Tisch, H. Haick, Nano Lett. 9 (2009) 1362.
[8] U.J. Kim, H.B. Son, E.H. Lee, J.M. Kim, S.C. Min, W. Park, Appl. Phys. Lett. 97 (2010) 032117.
[9] A. Gohier, A. Dhar, L. Gorintin, P. Bondavalli, Y. Bonnassieux, C.S. Cojocaru, Appl. Phys. Lett. 98 (2011) 063103.
[10] M.E. Roberts, M.C. LeMieux, Z. Bao, ACS Nano 3 (2009) 3287.
[11] M.Y. Zavodchikova, A.G. Nasibulin, T. Kulmala, K. Grigoras, A.S. Anisimov, S. Franssila, V. Ermolov, E.I. Kauppinen, Phys. Status Solidi B 245 (2008) 2272.
[12] E.Y. Jang, T.J. Kang, H.W. Im, D.W. Kim, Y.H. Kim, Small 4 (2008) 2255.
[13] A.H. Monica, S.J. Papadakis, R. Osiander, M. Paranjape, Nanotechnology 19 (2008) 085303.
[14] X. Xiong, L. Jaberansari, M.G. Hahm, A. Busnaina, Y.J. Jung, Small 3 (2007) 2006.
[15] Y. Liu, S. Lu, B. Panchapakesan, Nanotechnology 20 (2009) 035203.
[16] Y. Wang, Z. Zhou, Z. Yang, X. Chen, D. Xu, Y. Zhang, Nanotechnology 20 (2009) 345502.
[17] H.C. Yuan, B. Yang, J.M. Simmons, M.S. Marcus, Z. Ma, M.A. Eriksson, M.G. Lagally, Proc. SPIE 5971 (2005) 597118.
[18] Q. Cao, S.H. Hur, Z.T. Zhu, Y.G. Sun, C.J. Wang, M.A. Meitl, M. Shim, J.A. Rogers, Adv. Mater. 18 (2006) 304.
[19] Y.J. Jung, Y. Homma, T. Ogino, Y. Kobayashi, D. Takagi, B. Wei, R. Vajtai, P.M. Ajayan, J. Phys. Chem. B 107 (2003) 6859.
[20] I.J. Teng, K.L. Chen, H.L. Hsu, S.R. Jian, L.C. Wang, J.H. Chen, W.H. Wang, C.T. Kuo, J. Phys. D Appl. Phys. 44 (2011) 145401.
[21] M.S. Dresselhaus, G. Dresselhaus, R. Satio, A. Jorio, Phys. Rep. 409 (2005) 47 (and references therein).
[22] V. Skákalová, A.B. Kaiser, Y.S. Woo, S. Roth, Phys. Rev. B 74 (2006) 085403.
[23] U.J. Kim, K.H. Kim, K.T. Kim, Y.S. Min, W. Park, Nanotechnology 19 (2008) 285705.
[24] T. Fukao, S. Nakamura, H. Kataura, M. Shiraishi, Jpn. J. Appl. Phys. 45 (2006) 6524.
[25] P.G. Collins, K. Bradley, M. Ishigami, A. Zett, Science 287 (2000) 1801.
[26] G.U. Sumanasekera, C.K.W. Adu, S. Fang, P.C. Eklund, Phys. Rev. Lett. 85 (2000) 1096.
[27] S.H. Jhi, S.G. Louie, M.L. Cohen, Phys. Rev. Lett. 85 (2000) 1710.
[28] D. Kang, N. Park, J. Hyun, E. Bae, J. Ko, J. Kim, W. Park, Appl. Phys. Lett. 86 (2005) 093105.
[29] S. Heinze, J. Tersoff, R. Martel, V. Derycke, J. Appenzeller, Ph. Avouris, Phys. Rev. Lett. 89 (2002) 106801.
[30] V. Derycke, R. Martel, J. Appenzeller, Ph. Avouris, Appl. Phys. Lett. 80 (2002) 2773.
[31] L. Qu, F. Du, L. Dai, Nano Lett. 8 (2008) 2682.
[32] C.M. Lin, W. Fang, Nanotechnology 20 (2009) 465502.